3-Year Follow-Up of Radiation-Associated Changes in Diastolic Function by Speckle Tracking Echocardiography

Tuohinen, Suvi Sirkku

2021-06

Tuohinen , S S , Skyttä , T , Huhtala , H , Poutanen , T , Virtanen , V , Kellokumpu-Lehtinen , P-L & Raatikainen , P 2021 , ' 3-Year Follow-Up of Radiation-Associated Changes in Diastolic Function by Speckle Tracking Echocardiography ' , JACC: Cardiooncology , vol. 3 , no. 2 , pp. 277-289 . https://doi.org/10.1016/j.jaccao.2021.03.005

http://hdl.handle.net/10138/333420
https://doi.org/10.1016/j.jaccao.2021.03.005

JACC: CARDIOONCOLOGY VOL. 3, NO. 2, 2021

ORIGINAL RESEARCH

3-Year Follow-Up of Radiation-Associated Changes in Diastolic Function by Speckle Tracking Echocardiography

Suvi Sirkku Tuohinen, MD, PhD,[a,b] Tanja Skyttä, MD, PhD,[c,d] Heini Huhtala, MSc,[e] Tuija Poutanen, MD, PhD,[f,g] Vesa Virtanen, MD, PhD,[b,d] Pirkko-Liisa Kellokumpu-Lehtinen, MD, PhD,[c,d] Pekka Raatikainen, MD, PhD[a]

ABSTRACT

BACKGROUND Radiation therapy (RT) results in myocardial changes consisting of diffuse fibrosis, which may result in changes in diastolic function.

OBJECTIVES The aim of this study was to explore RT-associated changes in left ventricular (LV) diastolic function.

METHODS Sixty chemotherapy-naive patients with left-sided, early-stage breast cancer were studied with speckle tracking echocardiography at 3 time points: prior to, immediately after, and 3 years after RT. Global and regional early diastolic strain rate (SRe) were quantified, as were parameters of systolic function.

RESULTS Regional changes in SRe, particularly the apical and anteroseptal segments, were observed over time and were more evident than global changes. The apical SRe declined from a median of 1.24 (interquartile range: 1.01 to 1.39) s^{-1} at baseline to 1.02 (interquartile range: 0.79 to 1.15) s^{-1} at 3 years of follow-up ($p < 0.001$). This decline was associated with the left ventricular maximal radiation dose ($\beta = 0.36$, $p = 0.007$). The global SRe was <1.00 s^{-1} (SRe_{dep}) in 11 (18.3%) patients at baseline, 21 (35%) patients ($p = 0.013$) post-RT, and 17 (28.3%) patients ($p = 0.051$) at 3 years. SRe_{dep} post-RT was independently associated with baseline cardiac abnormalities (odds ratio: 0.26; 95% confidence interval: 0.08 to 0.84; $p = 0.025$); SRe_{dep} at 3 years of follow-up was associated with the baseline Charlson comorbidity index (odds ratio: 2.36; 95% confidence interval: 1.17 to 4.77; $p = 0.017$). Diastolic function abnormalities were evident even in patients with preserved global longitudinal strain at 3 years.

CONCLUSIONS RT resulted in changes in the SRe in the apical and anteroseptal segments over 3 years of follow-up. Changes in SRe apical segments were present even in patients with preserved systolic function and were independently associated with RT dose and cardiovascular comorbidities. (J Am Coll Cardiol CardioOnc 2021;3:277–89) © 2021 The Authors. Published by Elsevier on behalf of the American College of Cardiology Foundation. This is an open access article under the CC BY-NC-ND license (http://creativecommons.org/licenses/by-nc-nd/4.0/).

From the [a]Heart and Lung Center, Helsinki University Central Hospital, Helsinki University, Helsinki, Finland; [b]Heart Hospital, Tampere University Hospital, University of Tampere, Tampere, Finland; [c]Department of Oncology, Tampere University Hospital, Tampere, Finland; [d]Faculty of Medicine and Health Technology, Tampere University, Tampere, Finland; [e]Faculty of Social Sciences, Tampere University, Tampere, Finland; [f]Center for Child Health Research, Tampere, Finland; and the [g]Department of Pediatrics, Faculty of Medicine and Heath Technology, Tampere University Hospital and Tampere University, Tampere, Finland. The authors attest they are in compliance with human studies committees and animal welfare regulations of the authors' institutions and Food and Drug Administration guidelines, including patient consent where appropriate. For more information, visit the Author Center.

Manuscript received May 3, 2020; revised manuscript received March 21, 2021, accepted March 21, 2021.

ISSN 2666-0873 https://doi.org/10.1016/j.jaccao.2021.03.005

ABBREVIATIONS AND ACRONYMS

ΔGLS15 = relative decline of more than 15% in global longitudinal strain

CI = confidence interval

DLV_{max} = maximal left ventricular radiation dose

GLS = global longitudinal strain

IQR = interquartile range

LAVI = left atrial volume indexed to body surface area

LV = left ventricular

LVEF = left ventricular ejection fraction

RT = radiotherapy

SR = strain rate

SRe = early diastolic strain rate

SRe_{apex} = apical early diastolic strain rate

SRe_{dep} = global early diastolic strain rate <1 s^{-1}

SRs = systolic strain rate

Radiotherapy (RT) is used to reduce cancer recurrence and improve outcomes in patients with breast cancer. However, the effects of RT are not limited to tumor, as RT may induce adverse effects in healthy tissue. Cardiac adverse effects (e.g., coronary stenosis, valvular lesions, pericardial constriction, rhythm and conduction abnormalities) increase long-term cardiac morbidity by 2-fold and heart failure risk by 7-fold (1,2). RT-induced diffuse myocardial fibrosis and thickening of the left ventricular (LV) wall may also result in heart failure with preserved ejection fraction (2).

Several groups have recently reported that RT impairs LV systolic function, as detected by strain echocardiography and cardiac magnetic resonance (3-6). As RT is postulated to result in myocardial fibrosis, and fibrosis is associated with diastolic dysfunction, we hypothesized that demonstration of early changes in diastolic function might provide new insights in the pathogenesis of RT-induced cardiac dysfunction (7). The aim of this prospective study was to explore the effects of RT on novel echocardiography-derived measures of LV global and regional early diastolic strain rates (SRe), and to further understand the relevance of these changes in the context of systolic function (8).

METHODS

PATIENT COHORT. Female patients with early-stage left-sided breast cancer were included in this single-center prospective study. The inclusion and exclusion criteria have been described previously (9). Briefly, eligible female patients with early-stage breast cancer were prospectively recruited. Exclusion criteria included second malignancy, severe lung disease, symptomatic heart failure, recent acute myocardial infarction (6 months), atrial fibrillation, pacemaker, left bundle branch block, severe psychiatric disorder, pregnancy or breast feeding, or under 18 or over 80 years of age. At baseline, the Charlson comorbidity index was calculated (10) and the following cardiac conditions were identified, which we postulated increased the vulnerability to RT-induced functional changes: a mildly dilated LV >54 mm in size in end-diastole, LV mass indexed to body surface area >100 g/m^2, ratio of early mitral inflow velocity and pulsed tissue Doppler early diastolic velocity >15, global longitudinal strain (GLS) >-15% (indicative of worse function), greater than mild valvular disease, and previous heart surgery or invasive coronary intervention. No patients were treated with chemotherapy due to the early stage of the disease. Clinical events including all-cause mortality and cardiovascular hospitalizations were collected over the follow-up time. The study complied with the Declaration of Helsinki, and the local ethical committee approved the protocol. All participants signed an informed consent form before enrollment.

RADIOTHERAPY. All patients received adjuvant conformal RT after breast cancer surgery between July 2011 and June 2013. A 3-dimensional treatment planning computed tomography with 3-mm slices was performed in a supine position in all patients. Optimal fields and shields were used to spare the heart from radiation as much as possible (**Figure 1**). RT was administered according to normal institutional clinical guidelines for a total of 50 Gy with 2-Gy fractions or for a total 42.56 Gy with 2.66-Gy fractions 5 days a week. Treatment contouring and planning were done with Eclipse v.10 system (Varian Medical Systems, Palo Alto, California). Dose volume histograms, including cardiac structures, were generated for each patient.

CARDIAC EXAMINATIONS. Patients were examined prior to RT (0 to 69 days), after the end of RT (0 to 8 days), and 3 years after RT (2.8 to 3.2 years). All echocardiography examinations were performed by the same cardiologist (S.S.T.) using a Philips iE33 ultrasound machine (Philips Healthcare, Bothell, Washington) and with a 1- to 5-MHz matrix-array X5-1 transducer according to a predefined protocol including apical 4-, 3-, and 2-chamber views optimized for strain analysis. All offline analyses were performed using Philips QLAB 10.1 by a single cardiologist blinded to cardiac RT dose. The SR curves for each individual segment were manually analyzed (**Figure 2**). In addition, a comprehensive evaluation of diastolic parameters was performed, with grading of diastolic function as per societal recommendations (11). Reproducibility for global, regional (4 horizontal regions including basal, mid, apical, and apex and 6 longitudinal regions including anterior, anteroseptal, inferoseptal, inferior, inferolateral, and anterolateral regions) and segmental (6 basal segments, 6 mid segments, 6 apical segments, each divided into anterior, anteroseptal, inferoseptal, inferior, inferolateral, and anterolateral segments, and 3 apex segments derived from 3 apical views) levels for SRe were analyzed in 20 healthy volunteers, the reproducibility values for systolic strain rates (SRs) have been reported previously (9). GLS was also measured to gain insight into systolic function. A relative

FIGURE 1 **Radiotherapy Fields in 3-Dimensional Computed Tomography Treatment Planning**

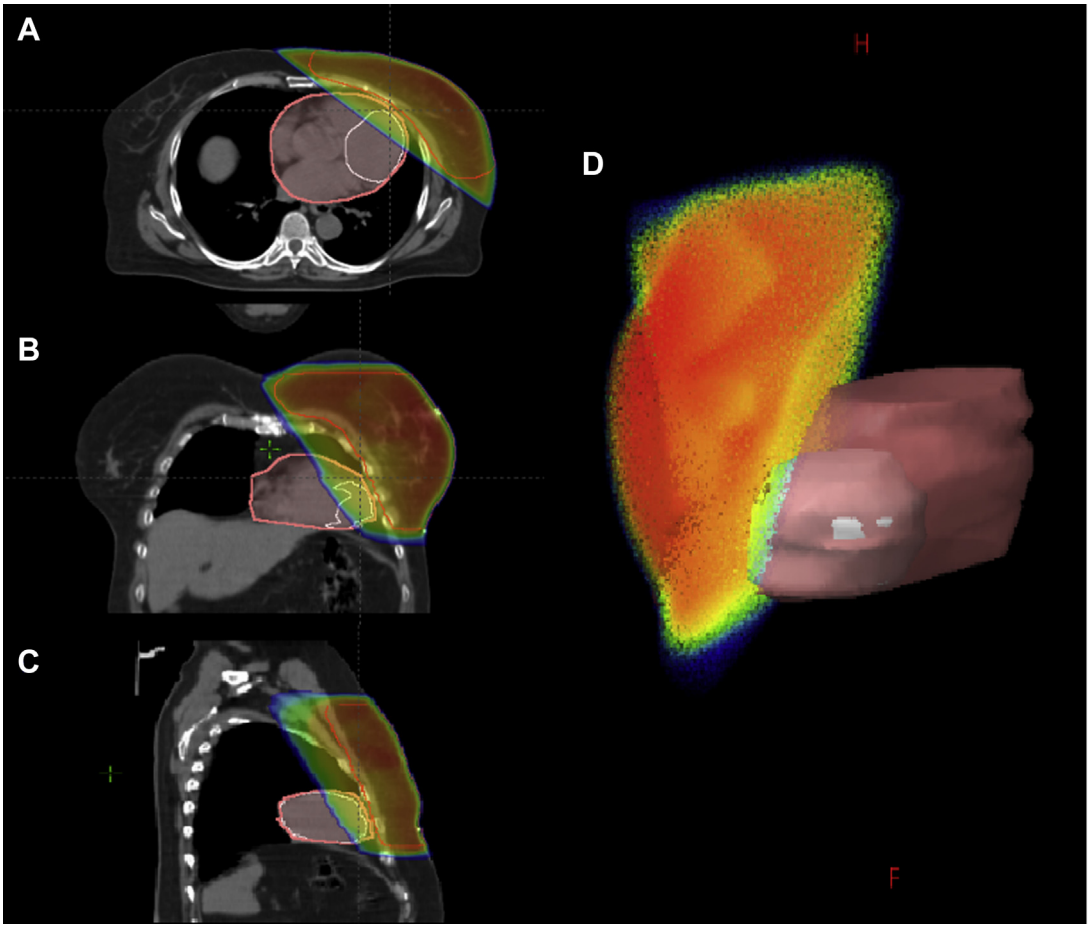

The treatment volume covered the remaining breast tissue after resection or left chest wall after mastectomy. Typically, the apical and anteroseptal parts of the heart were in the radiotherapy field, here as **yellow-orange fields** in 2-dimensional **(A)** axial, **(B)** coronal, and **(C)** sagittal images. **(D)** A 3-dimensional illustration is seen from the posterolateral view with apex and anterior parts of the heart imbedded in the colored radiotherapy field.

decline in GLS of 15% (ΔGLS15) at 3 years was defined as a clinically significant change as per guidelines (1).

FRAMERATE AND REPRODUCIBILITY ANALYSIS. All imaging was actively optimized for strain analysis, and the median frame rate was 69 (interquartile range [IQR]: 61 to 78) frames/s. The SRe intraclass correlation coefficient values with 95% confidence intervals (CIs) for intraobserver variability were 0.810 (95% CI: 0.520 to 0.925) for global values, 0.883 (95% CI: 0.864 to 0.912) for regional values, and 0.792 (95% CI: 0.747 to 0.828) for segmental values. The values for respective inter- and test-retest evaluations are shown in Supplemental Table 1.

STATISTICAL ANALYSIS. Data are presented as mean ± SD for variables with normal distributions, as median (IQR) for non-normally distributed variables, or as numbers with percentages for categorical variables. The differences between groups were tested with independent-sample *t* tests, Mann-Whitney U tests, and chi-square or Fisher's tests, as appropriate. To test the within group measurement changes over time, mixed-effects models were used. Patient was treated as a random factor and time as fixed. First-order autoregressive covariance structure was used to evaluate the repeated measures over time. Correlations were estimated using Pearson correlation coefficients. Multivariable linear regression analysis including age, use of aromatase inhibitors, current smoking status, maximal LV dose (DLV_{max}), Charlson comorbidity index, and subclinical or stable cardiac conditions was performed with

FIGURE 2 Measurement of Early Diastolic Strain Rate

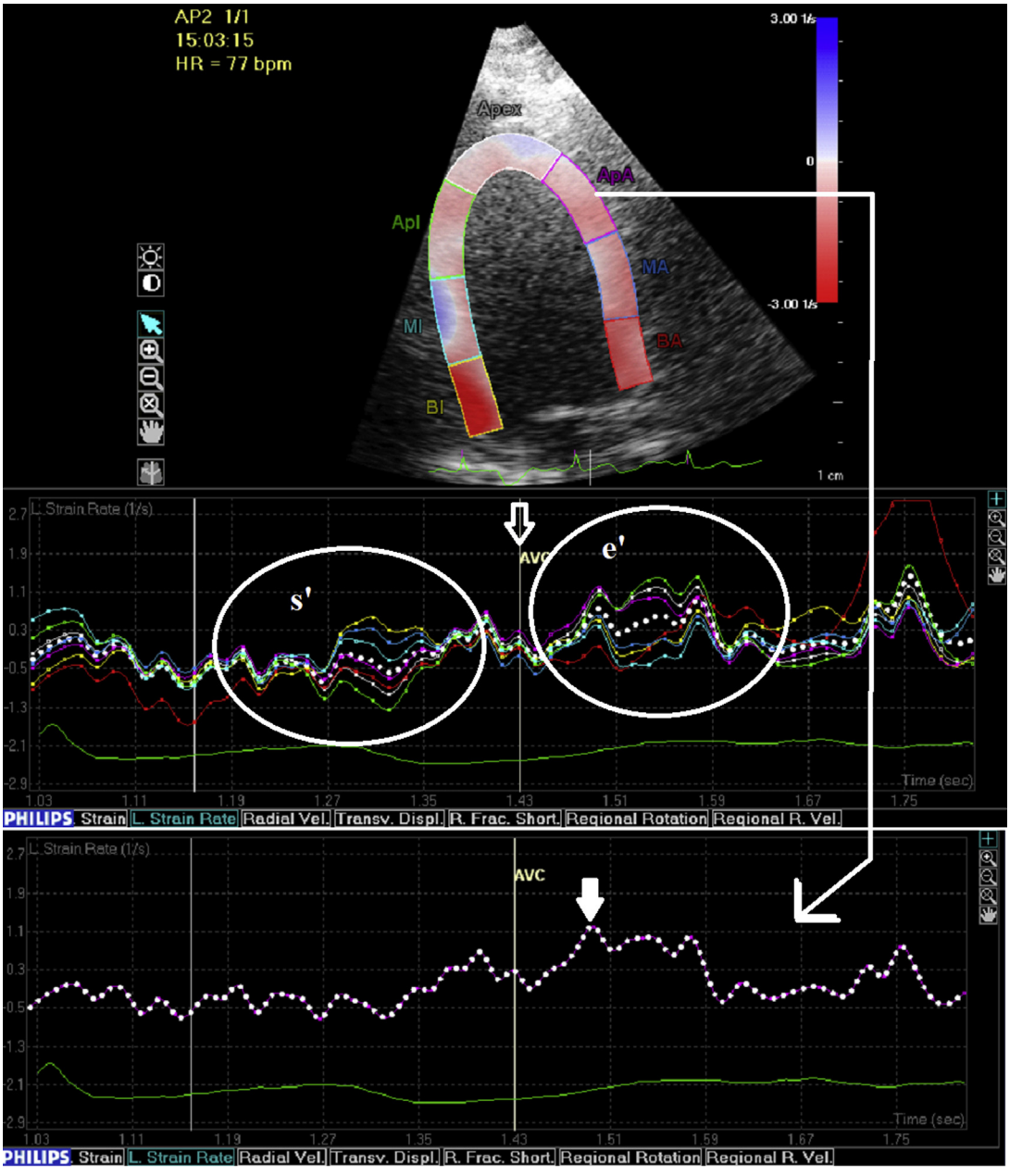

The apical 2-chamber view is presented on the **top of the image** with coloring over the myocardial segments. A cluster of strain rate curves is displayed in the **middle of the image**. Aortic valve closure (AVC) is marked with an **open white arrow**. The low point prior AVC is the systolic strain rate (s′) and the first high point after AVC is the early diastolic strain rate (e′). The **lowest part of the image** displays 1 individual segment (apical anterior [APA] segment). The **white arrow** indicates the exact measurement of the segmental early diastolic strain rate of the APA. API = apical inferior; BA = basal anterior; BI = basal inferior; MA = mid anterior; MI = mid inferior.

a forward stepwise method with SRe and SRs changes as the dependent variable; a binary logistic regression model was used with depressed SRe value at the 3-year follow-up time point as the dependent variable. For the reproducibility analysis, the intraclass correlation with 2-way random testing was used. The analysis was performed with IBM SPSS version 25 (IBM, Armonk, New York). Two-

TABLE 1 Baseline Characteristics of the Study Population (N = 60)

Age, yrs	64 (49-83)
BMI, kg/m^2	26.4 (19.7-40.8)
Smoker	9 (15.0)
CV risk factors	
Hypertension	22 (36.7)
Diabetes	4 (6.7)
High cholesterol	14 (23.3)
None	28 (53.3)
Subclinical and clinical CV disease	17 (28.3)
LVEDD >54 mm	2 (3.3)
GLS >-15%	7 (11.7)
E/e′ >15	3 (5.0)
LVMi >100 g/m^2	11 (18.3)
Greater than mild valvular abnormality	3 (5.0)
Prior heart surgery	1 (1.7)
Prior PCI	1 (1.7)
Charlson comorbidity index at baseline	
Points	4 (2-8)
2	1 (1.7)
3	19 (31.7)
4	25 (41.7)
5	11 (18.3)
6	2 (3.3)
7	1 (1.7)
8	1 (1.7)
Post-surgery breast cancer treatment	
Chemotherapy	
None	60 (100.0)
Radiotherapy	
Mean LV dose	4.4 (0.8-12.3)
Max LV dose	45.8 (4.5-63.8)
Mean heart dose	3.1 (0.7-6.8)
Hormonal therapy	
AI	22 (36.7)
Tamoxifen	2 (3.3)

Values are median (range) or n (%).

AI = aromatase inhibitor; BMI = body mass index; CV = cardiovascular; E/e′ = ratio of early mitral inflow velocity and pulsed tissue Doppler early diastolic velocity; GLS = global longitudinal strain; LV = left ventricular; LVEDD = left ventricular end-diastolic diameter; LVMi = left ventricular mass indexed to the body surface area; PCI = percutaneous coronary intervention.

sided p values <0.05 were considered statistically significant.

RESULTS

PATIENT CHARACTERISTICS. All 60 patients completed 3 years of follow-up. Seven (11.7%) patients were treated for a new or pre-existing cardiac disorder during the follow-up period. Two (3.3%) patients were treated for worsening of pre-existing heart condition (1 for acute coronary syndrome and 1 for aortic stenosis). One (1.7%) patient received a pacemaker for newly diagnosed sinus node dysfunction, 1 (1.7%) patient underwent catheter ablation for supraventricular tachycardia, and 3 (5%) patients were diagnosed with paroxysmal atrial fibrillation. The characteristics of the population are shown in Table 1.

GLOBAL SRs VALUES. Seven patients did not have quantitation of strain at the baseline due to missing data. Global SRs did not change significantly during follow-up (Table 2). Patients with ΔGLS15 at 3 years of follow-up (n = 16) had a SRs worsening to a median of 0.23 (IQR: 0.05 to 0.42) s^{-1} versus an increase by 0.04 (IQR: -0.10 to 0.13) s^{-1} in patients without ΔGLS15 (n = 39) (p = 0.001). In multivariable analysis, changes in global SRs during the 3-year follow-up were not associated with use of aromatase inhibitors, current smoking status, DLV_{max}, Charlson comorbidity index, or subclinical or stable cardiac conditions.

GLOBAL SRe VALUES. Global SRe declined from median 1.14 (IQR: 1.06 to 1.33) s^{-1} at baseline to 1.06 (IQR: 0.90 to 1.30) s^{-1} after RT (p = 0.084), and to 1.10 (IQR: 0.87 to 1.27) s^{-1} at 3 years (p = 0.069). SRe was <1.00 s^{-1} (SRe_{dep}) in 11 (18.3%) patients at baseline, in 21 (35.0%) patients post-RT (p = 0.013), and in 17 (28.3%) patients at 3 years (p = 0.051). In multivariable analysis, SRe_{dep} was not associated with any baseline covariates. Immediately after RT, SRe_{dep} was associated with baseline subclinical cardiac abnormalities (odds ratio: 0.26; 95% CI: 0.08 to 0.84; p = 0.025). At 3 years, the baseline Charlson comorbidity index was associated with SRe_{dep} (odds ratio: 2.36; 95% CI: 1.17 to 4.77; p = 0.017). The global SRe at 3 years was 1.01 (IQR: 0.87 to 1.32) and 1.10 (IQR: 0.88 to 1.27) among patients with and without a cardiac event during the follow-up, respectively, which was not significantly different (p = 0.658). SRe_{dep} was not more prevalent among those who experienced a cardiac event at 3 years (p = 0.407).

REGIONAL SRs VALUES. Regional basal SRs values are illustrated in Table 2. In patients with ΔGLS15, the SRs apex worsened by 0.38 (IQR: 0.17 to 0.53) s^{-1}, while in patients without ΔGLS15, SRs apex changed by only 0.01 (IQR: -0.15 to 0.10) s^{-1} (p < 0.001). In multivariable analysis, the Charlson comorbidity index was independently associated with the change in SRs apex at the 3-year follow-up time point (β = -0.17; 95% CI: -0.33 to -0.01; p = 0.044).

REGIONAL SRe VALUES. The regional SRe changes are shown in Table 2 and in the Central Illustration. The apex SRe (SRe_{apex}) had the greatest overall decline throughout the follow-up period; this was by -0.18 (IQR: -0.48 to 0.04) s^{-1}. In multivariable analysis, the DLV_{max} was independently associated with Δ SRe_{apex} (β = 0.01, (95% CI: 0.00 to 0.02; p = 0.007).

TABLE 2 Global and Regional Strain Rates

	Baseline (n = 53)	After RT (n = 58)	3-Year Follow-Up (n = 60)	p Value
Systolic				
Global	-1.25 (-1.45 to -1.11)	-1.30 (-1.45 to -1.11)	-1.27 (-1.40 to -1.14)	0.639
Basal	-1.46 (-1.75 to -1.17)	-1.62 (-1.87 to -1.37)*	-1.58 (-1.85 to -1.33)	0.057
Mid	-1.26 (-1.64 to -1.09)	-1.38 (-1.60 to -1.09)	-1.34 (-1.59 to -1.10)	0.396
Apical	-1.09 (-1.29 to -0.95)	-1.07 (-1.24 to -0.92)	-1.04 (-1.16 to -0.90)†‡	0.013
Apex	-1.05 (-1.22 to -0.90)	-0.99 (-1.15 to -0.87)	-0.98 (-1.08 to -0.86)†‡	0.026
Anterior	-1.15 (-1.52 to -0.99)	-1.20 (-1.59 to -1.00)	-1.23 (-1.36 to -1.07)	0.349
Anteroseptal	-1.25 (-1.55 to -1.07)	-1.23 (-1.46 to -1.09)	-1.22 (-1.42 to -1.09)	0.888
Inferoseptal	-1.19 (-1.31 to -1.07)	-1.21 (-1.40 to -1.10)	-1.21 (-1.35 to -1.07)	0.514
Inferior	-1.31 (-1.54 to -1.14)	-1.39 (-1.72 to -1.16)	-1.23 (-1.43 to -1.06)‡	0.086
Inferolateral	-1.31 (-1.85 to -1.06)	-1.37 (-1.61 to -1.19)	-1.53 (-1.71 to -1.82)	0.252
Anterolateral	-1.31 (-1.80 to -1.07)	-1.32 (-1.59 to -1.12)	-1.36 (-1.67 to -1.15)	0.406
Early diastolic				
Global	1.14 (1.06 to 1.33)	1.06 (0.90 to 1.30)	1.10 (0.87 to 1.27)	0.053
Basal	1.06 (0.87 to 1.18)	1.06 (0.86 to 1.35)	0.99 (0.83 to 1.32)	0.417
Mid	1.14 (1.00 to 1.53)	1.14 (0.90 to 1.48)	1.21(0.85 to 1.41)	0.569
Apical	1.25 (1.04 to 1.43)	1.08 (0.95 to 1.33)	1.05 (0.86 to 1.18)	0.438
Apex	1.24 (1.01 to 1.39)	0.76 (0.62 to 0.99)†	1.02 (0.79 to 1.15)†§	<0.001
Anterior	1.21 (0.95 to 1.50)	1.16 (0.86 to 1.53)	1.19 (0.94 to 1.40)	0.714
Anteroseptal	1.22 (0.93 to 1.44)	1.07 (0.84 to 1.45)	0.98 (0.75 to 1.21)†§	0.008
Inferoseptal	1.21 (0.94 to 1.39)	1.12 (0.94 to 1.37)	1.11 (0.89 to 1.25)	0.170
Inferior	1.07 (0.79 to 1.40)	1.09 (0.85 to 1.38)	1.13 (0.81 to 1.38)	0.374
Inferolateral	1.17 (0.89 to 1.41)	1.18 (0.79 to 1.31)	1.13 (0.76 to 1.41)	0.368
Anterolateral	1.22 (0.90 to 1.44)	1.13 (0.89 to 1.41)	1.12 (0.85 to 1.34)	0.424

Values are median (interquartile range). Owing to missing primary data, strain analysis could not be performed in 7 patients at the baseline and in 2 patients after radiotherapy (RT). The p values were derived from mixed model analysis with values <0.05. *p < 0.05 compared with baseline radiotherapy value. †p < 0.01 compared with baseline radiotherapy value. ‡p < 0.05 compared with after radiotherapy value. §p < 0.01 compared with after radiotherapy value.

Each 1 Gy of DLV_{max} was associated with a Δ SRe_{apex} of -0.012 s^{-1}. The associations between Δ SRe_{apex} and various heart radiation dose-volume metrics are shown in **Figure 3**. The decline in SRe_{apex} was 0.18 (95% CI: 0.07 to 0.29) s^{-1} in patients without a clinical event and 0.25 (95% CI: -0.10 to 0.60) with a clinical event during the 3-year follow-up (p = 0.655).

SEGMENTAL SR VALUES. The segmental systolic (SRs) and diastolic (SRe) values are shown in **Table 3**. The changes in both were concentrated in the apical and anteroseptal regions.

CONVENTIONAL ECHOCARDIOGRAPHY MEASURES. The results of conventional echocardiography are displayed in **Table 4**, and some of these results have been previously published (9). A worsening in GLS appeared early (p = 0.003) and persisted throughout the 3-year follow-up period (p = 0.001). There was an overall worsening of 1.7 ± 3.5%. A late reduction in the LV ejection fraction (LVEF) (p < 0.001), late increases in the tricuspid regurgitation gradient (p = 0.016), and left atrial volume indexed to body surface area (LAVI) (p = 0.003) were observed at 3 years. LVEF declined by 5.2 ± 9.8% from baseline to 3 years, the tricuspid gradient increased by 2.0 ± 5.4 mm Hg, and the LAVI increased by 2.1 ± 6.9 ml.

The changes of individual diastolic parameters for the entire cohort are presented in **Table 4**. Patients were graded as normal, grade 1 (abnormal relaxation), grade 2 (pseudonormal filling), or grade 3 (restrictive filling) diastolic dysfunction. The results of diastolic grading are presented in Supplemental Figure 1. Forty-three (71.6%) patients had no change in diastolic grade, while 14 (23.3%) patients displayed worsening and 3 (5.0%) patients had improved diastolic grade at 3 years compared with baseline.

CHANGES IN DIASTOLIC FUNCTION MEASURES ACCORDING TO CHANGES IN GLS. The diastolic function parameters categorized according to ΔGLS15 are presented in **Table 5**. Patients with ΔGLS15 at 3 years (n = 16) had greater changes in diastolic parameters over the same time period compared with patients without a significant change in GLS at 3 years (n = 37). In patients with a ΔGLS15 at 3 years, the global SRe declined by a median of 0.25 (IQR: 0.05 to 0.47) s^{-1}. In contrast, in patients without a ΔGLS15, the global SRe only declined by 0.05 (IQR: -0.13 to 0.18) s^{-1}

($p = 0.043$ for between-group differences). In patients without a significant change in GLS, the early mitral inflow velocity declined by 4 (IQR: -3 to 11) cm/s ($p = 0.013$), and the declaration time of the early mitral inflow slope was prolonged by 20 (IQR: -14 to 58) ms ($p = 0.007$); in contrast, patients with ΔGLS15 had a stable early mitral inflow velocity ($p = 0.650$) and declaration time of the early mitral inflow slope ($p = 0.008$) that was shortened by a median of -39 (IQR: -68 to -17) ms. Furthermore, in patients with ΔGLS15, the global SRe declined ($p = 0.020$), the LAVI increased ($p = 0.061$), and the tricuspid regurgitation gradient increased ($p = 0.005$) by 0.3 (IQR: 0.1 to 0.5) s^{-1}, 4 ± 10 ml, and 7.1 ± 5.6 mm Hg, respectively. There was a reduction in SRe_{apex} in those without ΔGLS15 ($p = 0.051$) with a decline of 0.1 (IQR: -0.1 to 0.4) s^{-1}; however, the change in patients with ΔGLS15 ($p = 0.017$) was worse, with a reduction of 0.4 (IQR: 0.1 to 0.7) s^{-1}.

DISCUSSION

Chest RT is associated with changes in diastolic function and heart failure with preserved ejection fraction (2,7). Our study supports these findings, as SRe changes appeared early and were more consistent than were changes in SRs. We also found that worsening diastolic function was detectable even in patients without significant changes in systolic function, as determined by GLS.

RT-INDUCED FIBROSIS. Biomarker studies, histologic studies, and cardiac positron emission tomography have shown that the early-phase RT-induced cardiac damage is characterized by microvascular inflammation and oxidative stress (7,12,13). Endothelial damage leads to capillary thrombosis, capillary vessel rarefication, and myocardial perfusion defects in the areas within the RT fields (14,15). Once initiated, the process may continue, leading to progressive accumulation of diffuse fibrosis and cell atrophy (15,16), which may lead to the myocardial thickening and restrictive diastolic function (7,17,18). In a study by Saiki et al. (2), 8% of breast cancer patients treated with RT developed heart failure within 6 years. Heart failure was predominantly diastolic, and the risk for heart failure with preserved ejection fraction increased by 16-fold after RT (2). In another study by Saiki et al. (7), evidence of RT was associated with changes in hemodynamics indicating increased LV stiffness, impaired relaxation, and higher LV end-diastolic pressure without changes in systolic function (7). These changes were more pronounced in patients receiving higher radiation doses, and were absent in nonradiated subjects.

CENTRAL ILLUSTRATION Radiotherapy-Associated Changes in Left Ventricular Strain Rate Over 3 Years

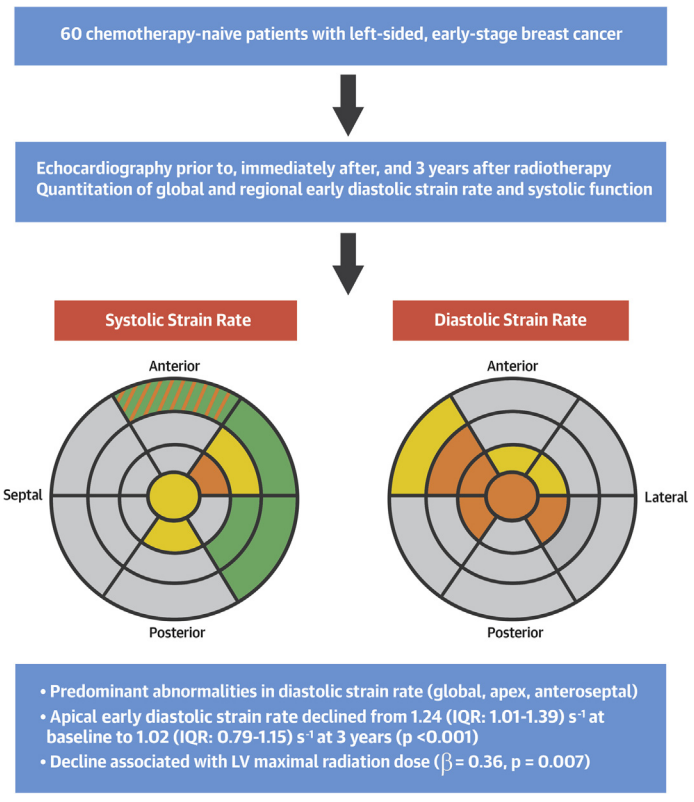

Tuohinen, S.S. et al. J Am Coll Cardiol CardioOnc. 2021;3(2):277–89.

A bullseye configuration of the left ventricle (LV) and change in for changes in systolic and early diastolic strain rate. The **middle of the image** presents the LV apex circled by apical, mid, and basal segments from middle to the outer layers, respectively. **Green** indicates improved function, while **yellow and orange** show worsening of the function in 1 or several follow-up visits, respectively. The worsening in diastolic strain rate is greater than the changes in systolic strain rate. The **green area with orange lines** indicate that this segment had both a significant increase (baseline to post-RT) and decrease (post-RT to 3-year control). IQR = interquartile range.

RT-INDUCED CHANGES IN CONVENTIONAL MEASURES OF DIASTOLIC FUNCTION. The early phase of LV filling is determined by LV relaxation and LV filling pressures. In conventional echocardiography, the evaluation of diastolic function is a complex task involving several parameters, by which diastolic function can be graded as normal or abnormal, according to grades 1 to 3 (11). Studies of post-RT changes using echocardiography have usually focused on changes in systolic function, and detailed data on multiple diastolic function parameters are lacking (5,9).

In our study, some of the diastolic parameters worsened during the 3 years of follow-up across the entire cohort. However, in the majority of the patients (n = 46, 67.8%) diastolic grade was not

FIGURE 3 Associations Between Apex SRe and Heart Radiation Dose

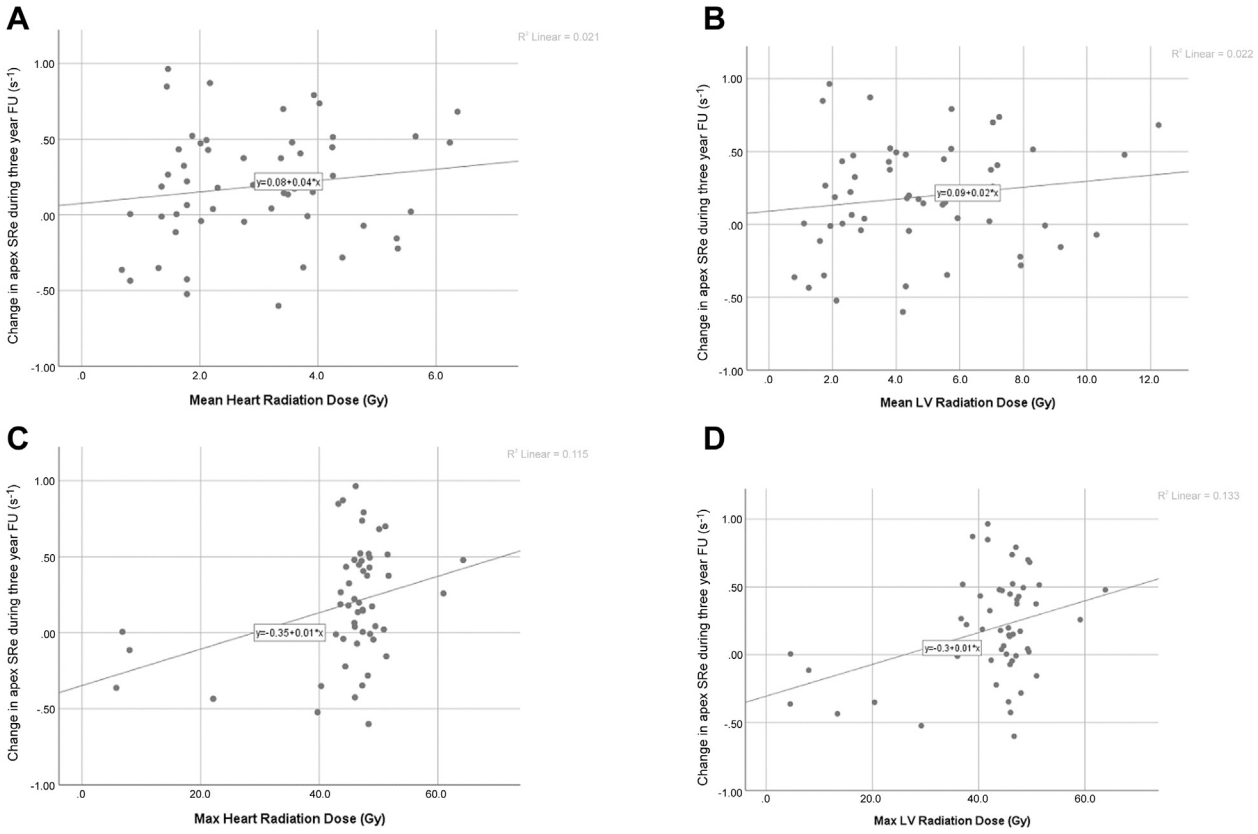

(A, C, E, G) The whole heart dose; **(B, D, F, H)** left ventricular dose. From **top to bottom**, **(A, B)** mean and **(C, D)** maximal doses and volumes receiving more than **(E, F)** 45 Gy and **(G, H)** 20 Gy radiation doses. FU = follow-up; SRe = early diastolic strain rate.

Continued on the next page

worsened. This might be secondary to diastolic grade being a combination of several measurements, which are affected by multiple factors.

Individual parameters of diastolic function also changed over time as the LAVI and tricuspid regurgitant gradient increased. In categorizing patients according to changes in GLS, a more precise pattern was recognized. Patients with and without ΔGLS15 displayed different changes in conventional diastolic parameters. Patients without a ΔGLS15 showed reduced mitral inflow E-wave and prolonged declaration times during the 3-year follow-up, indicating a shift toward relaxation abnormalities that may be more consistent with grade 1 diastolic dysfunction. In contrast, patients with ΔGLS15 had unchanged mitral inflow E waves but shorter declaration times, increased LAVIs, and increased tricuspid regurgitation gradients, potentially indicating a shift toward grade 2 to 3 diastolic dysfunction. These findings might suggest that these changes are indicators of RT-induced myocardial damage.

EARLY DIASTOLIC SR. Global SRe has been studied to understand increases in LV filling pressure and as a potential prognostic marker. In a study by Morris et al. (19), the normal range of global SRe in healthy subjects was 1.56 ± 0.28 s^{-1}, and SRe_{dep} was associated with a 5-fold increased risk of heart failure hospitalization. The global SRe has also been validated with invasive measurements of LV filling pressures (20–22).

Changes in SRe have been previously studied by Sritharan et al. (3), who showed a significant post-RT reduction over 6 weeks. In our study, the decline in global SRe was largely apparent in

FIGURE 3 Continued

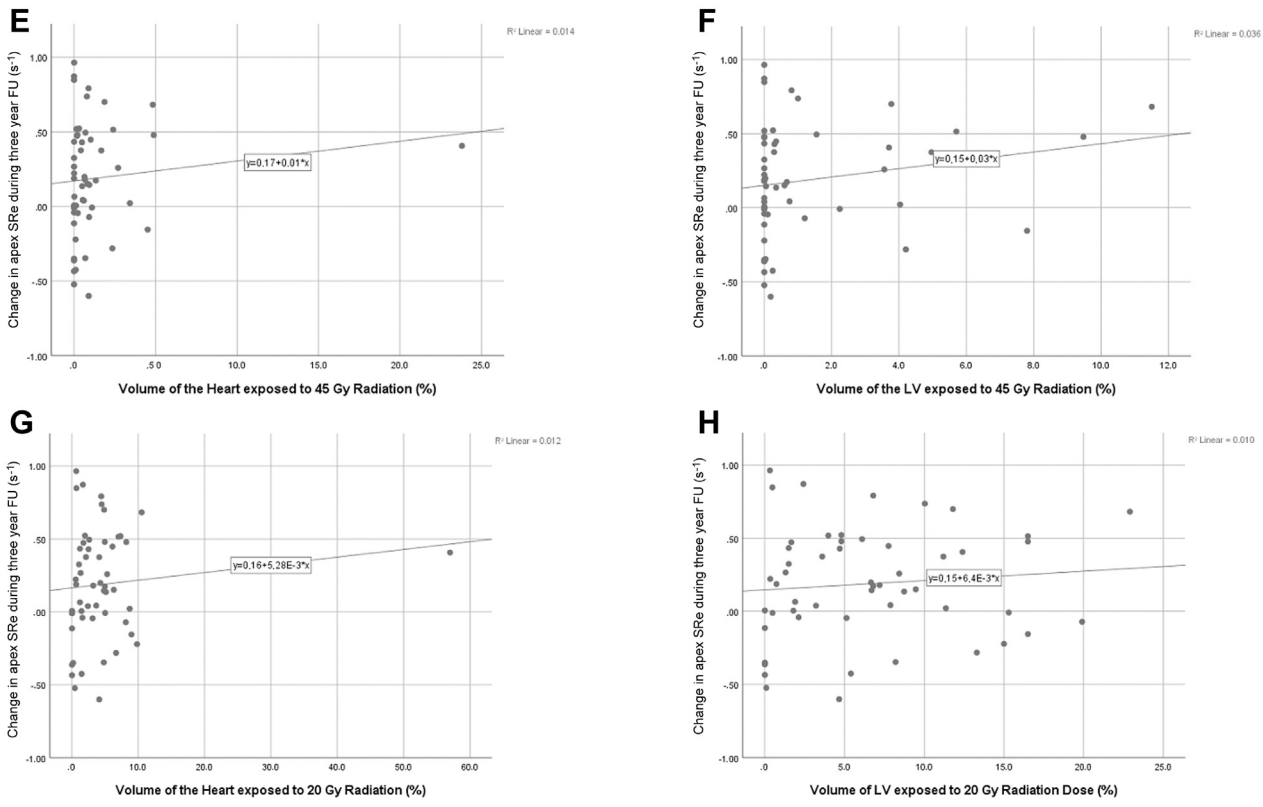

patients who also had a ΔGLS15. The number of patients with SRe_{dep} increased from 11 patients at baseline to 21 immediately after RT ($p = 0.013$) and to 17 at 3 years of follow-up ($p = 0.051$). The frequency of SRe_{dep} was highest immediately after RT, possibly related to the early effects of RT on very sensitive measures of cardiac function. In multivariable analysis, cardiac abnormalities at baseline were inversely associated with SRe_{dep} after RT. It may be that this association is confounded, and treatment for pre-existing heart disease had a protective effect to radiation in the early phase after RT. The baseline Charlson comorbidity index was independently associated with SRe_{dep} at 3 years. It is tempting to speculate that a pre-existing microvascular defect that worsens with age and other comorbidities would make the heart more vulnerable to RT-induced microvascular damage (2,13). In keeping with this, comorbidities were associated with SRe_{dep} and SRe_{apex} in our study.

The regional changes after RT in SRe were more evident than changes in global SR. The regional changes were concentrated in areas within the RT fields. According to our data and the results of a cross-sectional study by Taylor et al. (23), in patients with left-sided breast cancer, the LV apex and anterior parts of the heart receive the highest radiation dose from the contemporary tangential RT fields. In contrast, in patients with hypertension and cardiomyopathy, the regional SR decline tends to occur in basal areas (24,25). The distribution of the regional changes may help us to understand the underlying pathologic basis for these changes.

It remains unclear which RT dose-volume metrics are most strongly associated with abnormalities in cardiac function—mean heart dose, the overall volume of the heart in the RT fields, or the maximum dose? In a review by Niska et al. (26), high doses to small volumes were associated with worse outcomes early after RT, while in the long term, the mean heart dose was associated with increased cardiac mortality. In our study, DLV_{max} showed a stronger association with ΔSRe_{apex} than the mean dose or other radiation dose-volume metrics.

TABLE 3 Segmental Strain Rates

	Baseline (n = 53)	After RT (n = 58)	3-Year Follow-Up (n = 60)	p Value
Systolic				
Basal anterior	-1.41 (-1.91 to -0.96)	-1.78 (-2.15 to -1.13)*	-1.49 (-1.84 to -1.18)†	0.012
Basal anteroseptal	-1.29 (-1.78 to -1.05)	-1.31 (-1.90 to -1.08)	-1.46 (-1.86 to -1.10)	0.581
Basal inferoseptal	-1.10 (-1.28 to -0.90)	-1.13 (-1.44 to -0.91)	-1.08 (-1.22 to -0.87)	0.401
Basal inferior	-1.54 (-2.00 to -1.10)	-1.47 (-2.46 to -1.11)	-1.37 (-1.80 to -1.02)	0.202
Basal inferolateral	-1.39 (-1.98 to -1.00)	-1.57 (-2.22 to -1.09)	-1.98 (-2.50 to -1.22)*	0.029
Basal anterolateral	-1.53 (-2.09 to -1.26)	-1.74 (-2.28 to -1.39)	-1.97 (-2.51 to -1.44)‡	0.057
Mid anterior	-1.17 (-1.62 to -0.88)	-1.13 (-1.61 to -0.78)	-1.20 (-1.74 to -0.89)	0.967
Mid anteroseptal	-1.37 (-1.69 to -1.03)	-1.25 (-1.57 to -1.00)	-1.30 (-1.53 to -0.96)	0.532
Mid inferoseptal	-1.17 (-1.43 to -1.01)	-1.23 (-1.40 to -1.00)	-1.17 (-1.33 to -0.98)	0.361
Mid inferior	-1.22 (-1.48 to -0.95)	-1.36 (-1.75 to -1.06)	-1.18 (-1.63 to -0.91)	0.133
Mid inferolateral	-1.34 (-1.86 to -1.06)	-1.18 (-1.54 to -0.93)	-1.34 (-2.09 to -1.04)†	0.047
Mid anterolateral	-1.43 (-2.00 to -0.99)	-1.20 (-1.73 to -0.80)‡	-1.33 (-2.08 to -0.99)	0.076
Apical anterior	-0.89 (-1.23 to -0.71)	-0.90 (-1.13 to -0.66)	-0.84 (-1.04 to -0.65)	0.180
Apical anteroseptal	-0.96 (-1.33 to -0.81)	-1.02 (-1.24 to -0.72)	-0.98 (-1.27 to -0.80)	0.910
Apical inferoseptal	-1.23 (-1.45 to -1.10)	-1.29 (-1.52 to -1.06)	-1.28 (-1.52 to -1.10)	0.957
Apical inferior	-1.22 (-1.38 to -1.08)	-1.16 (-1.37 to -0.99)	-1.04 (-1.32 to -0.86)*	0.017
Apical inferolateral	-1.29 (-1.50 to -1.03)	-1.18 (-1.36 to -0.97)	-1.12 (-1.27 to -0.92)	0.108
Apical anterolateral	-0.96 (-1.18 to -0.72)	-0.91 (-1.19 to -0.70)	-0.82 (-1.00 to -0.68)†‡	0.041
Apex (4 chamber)	-1.06 (-1.23 to -0.84)	-1.02 (-1.23 to -0.88)	-1.05 (-1.14 to -0.85)	0.441
Apex (3 chamber)	-0.98 (-1.30 to -0.86)	-0.91 (-1.14 to -0.78)	-0.88 (-1.08 to -0.75)*	0.028
Apex (2 chamber)	-1.05 (-1.31 to -0.82)	-0.98 (-1.23 to -0.82)	-0.97 (-1.12 to -0.80)	0.227
Early diastolic				
Basal anterior	1.11 (0.62 to 1.64)	1.12 (0.81 to 1.62)	1.09 (0.73 to 1.64)	0.923
Basal anteroseptal	0.92 (0.53 to 1.27)	1.10 (0.66 to 1.55)	0.81 (0.43 to 1.19)§	0.036
Basal inferoseptal	0.85 (0.58 to 1.18)	0.77 (0.56 to 1.09)	0.80 (0.45 to 1.07)	0.328
Basal inferior	0.94 (0.55 to 1.40)	1.14 (0.72 to 1.55)	1.09 (0.62 to 1.56)	0.407
Basal inferolateral	1.18 (0.73 to 1.51)	1.07 (0.47 to 1.52)	1.01 (0.56 to 1.46)	0.258
Basal anterolateral	1.12 (0.84 to 1.60)	1.15 (0.72 to 1.58)	1.25 (0.64 to 1.68)	0.816
Mid anterior	1.18 (0.80 to 1.89)	1.20 (0.60 to 1.83)	1.25 (0.73 to 1.83)	0.635
Mid anteroseptal	1.29 (1.01 to 1.70)	1.23 (0.69 to 1.98)	0.91 (0.62 to 1.50)†‡	0.056
Mid inferoseptal	1.16 (0.84 to 1.54)	1.10 (0.92 to 1.40)	1.12(0.89 to 1.47)	0.984
Mid inferior	0.98 (0.69 to 1.50)	0.94 (0.70 to 1.43)	0.97 (0.63 to 1.52)	0.858
Mid inferolateral	0.97 (0.64 to 1.32)	1.01 (0.62 to 1.60)	1.14 (0.56 to 1.64)	0.565
Mid anterolateral	1.08 (0.70 to 1.72)	0.98 (0.58 to 1.57)	1.04 (0.66 to 1.56)	0.329
Apical anterior	1.07 (0.74 to 1.48)	0.82 (0.60 to 1.25)*	0.99 (0.68 to 1.32)	0.032
Apical anteroseptal	1.20 (0.75 to 1.56)	1.02 (0.65 to 1.22)‡	0.99 (0.72 to 1.24)‡	0.041
Apical inferoseptal	1.44 (1.00 to 1.97)	1.48 (1.07 to 1.69)	1.28 (0.97 to 1.62)†‡	0.063
Apical inferior	1.22(0.84 to 1.59)	1.05 (0.80 to 1.41)	0.99 (0.74 to 1.33)	0.377
Apical inferolateral	1.19 (0.90 to 1.64)	1.02 (0.73 to 1.42)‡	0.97 (0.68 to 1.25)*	0.009
Apical anterolateral	1.01 (0.79 to 1.50)	1.02 (0.72 to 1.51)	0.92 (0.62 to 1.20)†	0.061
Apex (4 chamber)	1.24 (0.93 to 1.66)	1.15 (0.91 to 1.40)	1.00 (0.76 to 1.37)*§	0.006
Apex (3 chamber)	1.21 (0.85 to 1.44)	0.94 (0.70 to 1.21)*	0.90 (0.69 to 1.29)*	0.008
Apex (2 chamber)	1.21 (0.84 to 1.54)	0.91 (0.65 to 1.30)*	0.93 (0.78 to 1.18)*	0.004

Values are median (interquartile range). Owing to missing primary data, strain analysis could not be performed in 7 patients at the baseline and in 2 patients after radiotherapy (RT). The p values were derived from mixed model analysis with values <0.05. *p < 0.01 compared with baseline radiotherapy value. †p < 0.05 compared with after radiotherapy value. ‡p < 0.05 compared with baseline radiotherapy value. §p < 0.01 compared with after radiotherapy value.

EARLY SYSTOLIC SR. Changes in SRs appeared later and were smaller than changes in SRe. However, similar to the changes in SRe and conventional diastolic function parameters, the changes in global SRs were more evident in patients with changes in GLS. As shown in our previous publications, GLS declined during follow-up (6,9). GLS is considered to be an earlier and more sensitive marker of changes in LV systolic function than LVEF, and a 15% relative decline is considered to present clinically significant deterioration (1). In our study, 16 patients experienced a significant ΔGLS15 during the 3 years of

TABLE 4 Conventional Echocardiography Parameters

	Baseline (n = 60)	After RT (n = 60)	3-Year Follow-Up (n = 60)	p Value
LVEDD, mm	45.1 ± 4.1	44.7 ± 3.9	45.2 ± 4.4	0.308
LVESD, mm	30.3 ± 3.5	30.0 ± 3.6	30.2 ± 3.5	0.766
LV mass, g	152 (137–174)	158 (139–186)*	154 (129–177)†‡	0.039
LVEF, %	64.6 ± 6.8	64.9 ± 7.3	59.4 ± 6.9†‡	<0.001
GLS, %	-18.3 ± 3.1	-17.3 ± 3.2§	-16.8 ± 3.1†	0.003
E, cm/s	72 (64–83)	67 (58–79)*	68 (61–81)	0.136
dt, ms	230 (203–260)	242 (207–271)	246 (203–279)	0.396
a, cm/s	78 ± 20	75 ± 15	75 ± 19	0.150
E/e′	8.9 (7.1–11.1)	8.5 (7.1–10.0)	9.3 (7.1–10.4)	0.237
e′ (septum)	7.4 (5.8–8.2)	7.0 (5.8–8.1)	6.9 (5.8–7.6)	0.119
e′ (lateral)	9.0 (7.3–11.8)	9.4 (7.2–10.6)	9.2 (7.7–10.4)	0.554
LAVI, ml/m^2	32.8 ± 8.4	32.3 ± 8.5	34.9 ± 8.7*‖	0.003
TAPSE, mm	24.2 ± 4.0	22.3 ± 4.0†	23.3 ± 4.3	<0.001
TR gradient, mm Hg	21.5 (19.0–25.0)	21.4 (19.5–24.5)	23.5 (19.8–27.0)*‖	0.016

Values are mean ± SD or median (interquartile range). *p < 0.05 compared with baseline radiotherapy value. †p < 0.001 compared with baseline radiotherapy value. ‡p < 0.001 compared with after radiotherapy value. §p < 0.01 compared with baseline radiotherapy value. ‖p < 0.05 compared with after radiotherapy value.

a = late diastolic mitral inflow velocity; dt = declaration time of the early inflow slope; E = early mitral inflow velocity; e′ = pulsed tissue Doppler early diastolic velocity of the basal myocardium; E/e′ = ratio of early mitral inflow velocity and pulsed tissue Doppler early diastolic velocity; LAVI = left atrial volume indexed to body surface area; LVEF = left ventricular ejection fraction, LVESD = left ventricular end-systolic diameter; TAPSE = tricuspid annular plane systolic excursion; TR gradient = tricuspid regurgitation maximal gradient; other abbreviations as in Tables 1 and 2.

follow-up. However, changes in diastolic function were also evident in patients without ΔGLS15, suggesting that changes in diastolic function may appear in the absence of detectable changes in systolic function.

STUDY LIMITATIONS. First, our sample size was small and from a single institution, limiting both our ability to adjust for multiple confounders and our power to detect significant associations, as well as the generalizability of our findings. The clinical adverse effects usually appear several years or decades after RT. Hence, longer follow-up time is needed to understand the clinical implications of these findings. Our study design also did not include a control group, making it difficult to exclude age or other factors that may have influenced the results. Moreover, there is an important and notable risk of type I error given the lack of correction for multiple testing, and as such, our results are hypothesis generating. The main technique used, SR analysis, is time-consuming. Before it can be applied to clinical practice, technological advancements and additional research are necessary. Furthermore, the overall usability in clinical practice may be lower than in the current study, as an experienced, echocardiography-focused cardiologist performed all the acquisition and analysis in

TABLE 5 Changes in Diastolic Function According to GLS Changes at 3 Years

	ΔGLS <-15% (n = 37)					ΔGLS >-15% (n = 16)					
	Baseline		3-Year Follow-Up			Baseline		3-Year Follow-Up			
	Median	IQR	Median	IQR	p_1 Value	Median	IQR	Median	IQR	p_1 Value	p_2 Value
Global SRe, s^{-1}	1.16	1.02–1.31	1.11	1.01–1.29	0.318	1.14	1.06–1.42	1.10	0.83–1.29	0.020	0.043
Apex SRe, s^{-1}	1.26	0.99–1.39	1.06	0.88–1.28	0.051	1.15	1.00–1.55	0.97	0.83–1.29	0.017	0.068
e′, s^{-1}	8.09	6.75,10.33	8.23	6.93–9.48	0.587	8.06	6.28–8.94	8.02	5.68–8.69	0.609	0.848
E, cm/s	71	64,85	67	61–81	0.013	66	60–78	69	62–81	0.650	0.222
dt, ms	224	194–250	246	225–291	0.007	256	208–288	222	169–254	0.008	<0.001
E/e′	8.7	6.8–10.9	8.3	6.8–10.3	0.118	9.2	6.7–11.5	8.9	8.1–9.9	0.394	0.186
LAVI, ml/m^2	33	25–38	33	28–39	0.323	36	30–40	39	31–42	0.061	0.084
TR gradient, mm Hg	21	18–25	22	19–24	0.379	22	21–27	27	26–32	0.005	<0.001

ΔGLS >-15% is indicative of worse systolic function. p_1 indicates the change in values from baseline to the 3-year follow-up. p_2 indicates the difference in the changes during the 3-year follow-up between the ΔGLS groups.

ΔGLS = change in global longitudinal strain during 3-year follow-up; IQR = interquartile range; SRe = early diastolic strain rate; other abbreviations as in Table 4.

the current study, and this resource might not be available in daily clinical practice.

CONCLUSIONS

Changes in diastolic function were detected early after RT and during 3 years of follow-up. These changes suggest a shift toward worsened relaxation patterns in breast cancer patients treated with RT. Regional SRe changes in RT-affected areas were detected in those with and without changes in systolic function, although they were more pronounced in those with a significant change in GLS.

ACKNOWLEDGMENTS The authors thank the research nurses Virpi Palomäki, Hanna-Leena Näppilä, Kati Helleharju, and Katri Mikkonen for their expert assistance during the study.

FUNDING SUPPORT AND AUTHOR DISCLOSURES

This study has received funding from nonprofit trusts: Paavo and Eila Salonen Legacy, the Finnish Foundation for Cardiovascular Research, and the Finnish Society of Oncology. The authors have reported that they have no relationships relevant to the contents of this paper to disclose.

ADDRESS FOR CORRESPONDENCE: Dr. Suvi Sirkku Tuohinen, Heart and Lung Center, Helsinki University Central Hospital and Helsinki University, PO Box 340, 00029 Helsinki, Finland. E-mail: suvi.tuohinen@fimnet.fi. Twitter: @tanjaskytta.

PERSPECTIVES

COMPETENCY IN MEDICAL KNOWLEDGE: In early-stage left-sided breast cancer patients treated with radiation therapy, changes in sensitive measures of LV diastolic function and early diastolic SR were observed, particularly in areas receiving high radiation dose.

TRANSLATIONAL OUTLOOK: Additional studies are needed to further define the changes in diastolic function that occur with radiation therapy and determine the relationship between changes in LV diastolic SR and adverse clinical outcomes.

REFERENCES

1. Zamorano JL, Lancellotti P, Rodriguez Muñoz D, et al. 2016 ESC Position Paper on cancer treatments and cardiovascular toxicity developed under the auspices of the ESC Committee for Practice Guidelines: The Task Force for cancer treatments and cardiovascular toxicity of the European Society of Cardiology (ESC). Eur Heart J 2016;37:2768–801.

2. Saiki H, Petersen IA, Scott CG, et al. Risk of heart failure with preserved ejection fraction in older women after contemporary radiotherapy for breast cancer. Circulation 2017;135:1388–96.

3. Sritharan HP, Delaney GP, Lo Q, et al. Evaluation of traditional and novel echocardiographic methods of cardiac diastolic dysfunction post radiotherapy in breast cancer. Int J Cardiol 2017;243:204–8.

4. Heggemann F, Grotz H, Welzel G, et al. Cardiac function after multimodal breast cancer therapy assessed with functional magnetic resonance imaging and echocardiography imaging. Int J Radiat Oncol Biol Phys 2015;93:836–44.

5. Trivedi SJ, Choudhary P, Lo Q, et al. Persistent reduction in global longitudinal strain in the longer term after radiation therapy in patients with breast cancer. Radiother Oncol 2019;132:148–54.

6. Erven K, Florian A, Slagmolen P, et al. Subclinical cardiotoxicity detected by strain rate imaging up to 14 months after breast radiation therapy. Int J Radiat Oncol Biol Phys 2013;85:1172–8.

7. Saiki K, Moulay G, Guenzel, et al. Experimental cardiac radiation exposure induces ventricular diastolic dysfunction with preserved ejection fraction. Am J Physiol Heart Circ Physiol 2017;313:H392–407.

8. Tuohinen SS, Skytta T, Huhtala H, et al. Left ventricular speckle tracking echocardiography changes among early-stage breast cancer patients three years after radiotherapy. Anticancer Res 2019;39:4227–36.

9. Tuohinen SS, Skytta T, Poutanen T, et al. Radiotherapy-induced global and regional differences in early-stage left-sided versus right-sided breast cancer patients: speckle tracking echocardiography study. Int J Cardiovasc Imaging 2017;34:191–8.

10. Charlson ME, Pompei P, Ales KL, et al. A new method of classifying prognostic comorbidity in longitudinal studies: development and validation. J Chronic Dis 1987;40:373–83.

11. Nagueh SF, Smiseth OA, Appleton CP, et al. Recommendations for the evaluation of left ventricular diastolic function by echocardiography: an update from the American Society Of Echocardiography and the European Association Of Cardiovascular Imaging. Eur Heart J Cardiovasc Imaging 2016;17:1321–60.

12. El-Sherif O, Xhaferllari I, Sykes J, et al. [18F] FDG cardiac PET imaging in a canine model of radiation-induced cardiovascular disease associated with breast cancer radiotherapy. Am J Physiol Heart Circ Physiol 2019;316:H586–95.

13. Franssen C, Chen S, Unger A, et al. Myocardial microvascular inflammatory endothelial activation in heart failure with preserved ejection fraction. J Am Coll Cardiol HF 2016;4:312–24.

14. Fajardo LF, Stewart JR. Pathogenesis of radiation-induced myocardial fibrosis. Lab Invest 1973;29:244–57.

15. Prosnitz RG, Hubbs JL, Evans ES, et al. Prospective assessment of radiotherapy-associated cardiac toxicity in breast cancer patients: analysis of data 3 to 6 years after treatment. Cancer 2007;110:1840–50.

16. Yarnold J, Brotons MC. Pathogenetic mechanisms in radiation fibrosis. Radiother Oncol 2010;97:149–61.

17. Umezawa R, Ota H, Takanami K, et al. MRI findings of radiation-induced myocardial damage in patients with oesophageal cancer. Clin Radiol 2014;69:1273–9.

18. Sardaro A, Petruzzelli MF, D'Errico MP, et al. Radiation-induced cardiac damage in early left breast cancer patients: Risk factors, biological mechanisms, radiobiology, and dosimetric constraints. Radiother Oncol 2012;103:133–42.

19. Morris DA, Takeuchi M, Nakatani S, et al. Lower limit of normality and clinical relevance of left ventricular early diastolic strain rate for the detection of left ventricular diastolic dysfunction. Eur Heart J Cardiovasc Imaging 2018;19:905–15.

20. Wang J, Khoury DS, Thohan V, et al. Global diastolic strain rate for the assessment of left

ventricular relaxation and filling pressures. Circulation 2007;115:1376–83.

21. Ma H, Wu WC, Xie RA, et al. Correlation of global strain rate and left ventricular filling pressure in patients with coronary artery disease: a 2-d speckle-tracking study. Ultrasound Med Biol 2016;42:413–20.

22. Chen S, Yuan J, Qiao S, et al. Evaluation of left ventricular diastolic function by global strain rate imaging in patients with obstructive hypertrophic cardiomyopathy: a simultaneous speckle tracking echocardiography and cardiac catheterization study. Echocardiography 2014;31:615–22.

23. Taylor C, McGale P, Bronnum D, et al. Cardiac structure injury after radiotherapy for breast cancer: cross-sectional study with individual patient data. J Clin Oncol 2018;36:2288–96.

24. Baltabaeva A, Marciniak M, Bijnens B, et al. Regional left ventricular deformation and geometry analysis provides insights in myocardial remodelling in mild to moderate hypertension. Eur J Echocardiogr 2008;9:501–8.

25. Trivedi S, Altman M, Stanton T, et al. Echocardiographic strain in clinical practice. Heart Lung Circ 2019;28:1320–30.

26. Niska JR, Thorpe CS, Allen SM, et al. Radiation and the heart: systematic review of dosimetry and cardiac endpoints. Expert Rev Cardiovasc Ther 2018;16:931–50.

KEY WORDS **breast cancer, diastolic strain rate, radiotherapy, speckle tracking echocardiography**

APPENDIX **For a supplemental table and figure, please see the online version of this paper.**